

PROPERTIES AND PREPARATION OF HIGH-PURITY ALUMINUM*

V. Arp
Cryogenics Division, Institute for Basic Standards
National Bureau of Standards
Boulder, Colorado

I. INTRODUCTION

The potential economy of using aluminum magnets operating at low temperatures was suggested by Post and Taylor¹ in 1959, before the advent of high field superconductivity. A liquid-hydrogen-cooled aluminum magnet was built and operated not long thereafter,² but by that time superconducting magnets seemed to be generally more attractive. Nevertheless, a small effort was carried on, since, for some low duty cycle conditions, aluminum appears to be more attractive than superconductors.^{3,4} We have continued a study of the properties of aluminum which are related to this type of application, and a major part of this paper summarizes this study and knowledge in a tutorial fashion. The final and minor section of the paper reports the current status on the availability of high-purity aluminum in technologically useful quantities.

II. PROPERTIES OF HIGH-PURITY ALUMINUM

In this, the major portion of the paper, electrical and thermal conductivities of metal are discussed, and data relevant to high-purity aluminum are presented. The analysis starts with a summary of various contributions to the dc resistivity. It then goes on to demonstrate the quantitative relationship between the electrical and thermal conductivities. Finally, it considers the response of metals under ac conditions.

1. The dc Resistivity of Metals

The customary approximation used in the discussion of the resistivity of metals is Mathiessen's rule

$$\rho \approx \sum_i \rho_i \quad , \quad (1)$$

where ρ_i is the "partial" resistivity due to any one mechanism which inhibits the flow of electrons through the metal. In the next approximation, one can find deviation terms to be added to the right side of Eq. (1)⁵; however, they will not be considered in this paper. Equation (1), then, forms the basis for separate discussions of various contributions to the total electrical resistivity of a metal.

Data on the electrical resistivity of aluminum as a function of temperature are summarized in Fig. 1.⁶ Starting at low temperature, samples of different purity are seen to have different resistivities, independent of temperature. This is the region where localized imperfections in the atomic lattice dominate the total resistivity; various types of imperfections, and the separate contributions to the total resistivity are discussed in Section 1.A. As the sample temperature is raised, the resistivity of all samples finally begins to rise, following a common or universal curve for this

*This work was carried out at the National Bureau of Standards under the sponsorship of the Department of the Army and the Department of the Air Force.

element. The temperature dependent resistivity is due to lattice vibrations, and is discussed in Section 1.B. The increase in resistivity for small sample sizes, not illustrated in Fig. 1, is discussed in Section 1.C.

1.A. Imperfection Resistivity

Imperfections in a metal can be divided into two general classes: impurities, which are discussed in 1.A.1., and lattice defects, which are discussed in 1.A.2. Lattice defects are further subdivided into (a) vacancies, (b) dislocations, and (c) grain boundaries.

1.A.1. Impurity resistivity. In close analogy with Eq. (1), the impurity resistivity can be written

$$\rho_{\text{impurities}} = \sum_i (\rho/c)_i c_i \quad (2)$$

where $(\rho/c)_i$ is a measure of the electron scattering by an isolated impurity atom of species i when substituted for a host atom in the lattice, and c_i is the concentration of the i atoms. Table I gives experimentally determined values of ρ/c for a variety of impurity atoms in aluminum.⁷⁻¹⁰ It must be emphasized that these data cannot be used at high concentrations or where the sample treatment has caused precipitation, segregation, or clustering of the impurity atoms.

TABLE I
Impurity Resistivity in Aluminum

Impurity	ρ/c ($10^{-12} \Omega \cdot \text{m/ppm}$)	"Partial resistivity ratio" for 1 ppm of impurity
Cr	8	3 300
Mo	7.5	3 500
Mn, V, W, Zr	7	3 800
Fe	6.5	4 100
Ti	6	4 400
Sc	5	5 300
Co	3.5	7 500
Ni	1.8	15 000
Ge, Ag, Cu, Pb, Li, Sb, Sn, Sb	≈ 1	$\approx 26\ 000$
Si, Zn As, Be, Mg	≤ 0.7	$\geq 38\ 000$

In practice, for all reasonably pure metals except mercury, the impurity resistivity is much larger than any other contribution to the total resistivity in the liquid helium range. Thus, the resistivity at 4°K is a direct measure of the total impurity content of the metal. It has become customary, however, to cite the "residual resistance ratio," (usually called just the "resistance ratio," or just "ratio") which is

$$\text{Residual resistance ratio} = \frac{R(20^\circ\text{C})}{R(4^\circ\text{K})}$$

where R is a measured sample resistance, rather than $\rho(4^{\circ}\text{K})$ as a measure of the sample purity. The last column of Table I gives the resistance ratio which would result from 1 ppm of the stated impurity in aluminum. We have been using $\rho(20^{\circ}\text{C}) = 2.64 \mu\Omega\cdot\text{cm} = 2.64 \times 10^{-8} \Omega\cdot\text{m}$.

For samples having resistance ratios in the range 1000 to 10 000, we have found excellent agreement (within 20%) between the measured resistivities and resistivities calculated using Eq. (2), Table I, and quantitative mass spectroscopic analysis. At higher resistivity ratios (higher purities), the calculated resistivities tend to be systematically higher than the measured resistivities, the disagreement being a factor of two for a 24 000-ratio sample. This certainly is due in part to the great difficulty of doing accurate mass spectrographic impurity analyses at less than 1 ppm total impurity concentration. We feel, however, that the systematic trend may be evidence for segregation of a fraction of impurities at grain boundaries where they would have less effect on the total resistivity than they would if randomly distributed throughout the sample. This will be discussed more carefully in Section 1.A.2.

A recent study on copper¹¹ contains evidence for the major effect which clustering of impurities can have on the resistivity ratio. By a suitable oxygenation technique they have been able to increase the resistivity ratio of copper from 2500 to 42 000 without removing the impurity atoms. They suggest that this is probably due to solute atom clustering or precipitation of impurity oxides, but neither has been verified. If the impurity oxide precipitation is responsible, however, the analogous procedure for aluminum would probably be ineffective, since aluminum oxide has a higher heat of formation than do the oxides of any expected impurities in aluminum. We have found no difference between aluminum annealed in air and aluminum annealed in a vacuum.

1.A.2. The lattice defect resistivity. A number of defects may occur in the atomic lattice arrangement of a metal. For the purposes of this paper, we may group them into three classes: (a) vacancies and/or interstitial atoms, (b) dislocations, which are linear regions where the atomic layers exhibit a slight misfit, and (c) grain boundaries, which separate regions (crystals) having completely different lattice orientations. Impurity atoms are often attracted to these defects, and so must be considered in certain aspects of the study.

Vacancies are formed spontaneously in a metal when it is heated to near its melting temperature, but a substantial portion will be retained at low temperatures only if the metal is quenched rather than being allowed to cool slowly. They are also formed at any temperature when the metal is strained beyond its elastic region. For aluminum, the vacancy resistivity is¹²:

$$\rho/c = 1.4 \times 10^{-12} \Omega\cdot\text{m}/\text{ppm} . .$$

We have found that vacancy concentration reaches equilibrium in high-purity aluminum at room temperature in just a few hours.

The resistivity due to dislocation structures in metals is a subject of active study at the present time,¹³⁻¹⁵ particularly in trying to find agreement between theory and experiment. The results depend to some extent on the type of dislocation and other factors which are beyond the scope of this paper. A reasonable estimate for aluminum comes from Rider and Foxon¹⁶:

$$\rho/n = 3 \times 10^{-25} \Omega\cdot\text{m}^3 ,$$

where n is the number of dislocation lines per square meter in the sample. We may reasonably expect no more than 10^{10} or 10^{11} dislocations/ m^2 in an annealed pure metal sample. After heavy deformation, this rises to a saturation value of roughly $10^{16}/\text{m}^2$ for most metals.

As with vacancies, dislocations are formed when a metal is strained beyond its elastic limit. Large uncertainties exist in trying to predict theoretically the number of vacancies or dislocations which are formed by a given strain.¹⁷ We have studied a portion of this problem with measurements on high-purity aluminum at low temperature. Samples were carefully prepared and annealed so as to be truly polycrystalline, since dislocation formation and structure are strongly dependent upon the relative orientation of the individual grains and the applied stress. Results obtained at 4°K on samples of about 2000 resistivity ratio are shown in Fig. 2, where the increase in resistivity is plotted against the strain ϵ which produced that resistivity.

These results are described approximately by the equation

$$\Delta\rho (10^{-11} \Omega\cdot\text{m}) = 110 \epsilon^{1.19}$$

It is reasonable to assume that minor changes in temperature or purity in the range of interest for cryogenic coils will not significantly change the numbers in this equation. Subsequent annealing of the samples at room temperature for a day or more results in the disappearance of about two-thirds of the strain-induced resistivity. We believe this is due to removal of vacancies and dislocation rearrangement. A much higher temperature, probably 300 to 400°C for one hour, would be necessary to eliminate the dislocations which are formed during straining.

Figure 3 shows the stress-strain curves which were taken simultaneously with the data of Fig. 2. It is difficult to estimate how the yield stress (about 3000 psi in these samples) would vary with purity in this high-purity range. It is, in fact, probably more strongly dependent upon grain size and orientation than on impurity content per se. The yield stress for annealed samples of 10³ higher impurity content (commercial 1100 aluminum) is only 2 to 3 times higher than that of these samples, so that a dramatic decrease in yield stress would not be expected as the resistivity ratio is increased from 2000 to the limit of available material. We will be making experimental measurements in this range in the near future. Fatigue life at stress levels below the yield stress would be very high, probably well into the 10⁶ to 10⁷ cycle range.

The resistivity due to grain boundaries has not been studied in much detail, and its direct effect is probably rather small, especially in high-purity metals where the grain size may be very large. However, impurities are in general attracted toward grain boundaries and may thus be removed from solid solution where they have maximum contribution to the sample resistivity. If we make the assumption that the saturation concentration of impurities at the grain boundaries corresponds to one atomic layer,¹⁸ this impurity trapping could become important when

$$(\text{impurity concentration in ppm}) \times (\text{grain diameter in mm}) \leq 2 .$$

In practice, for a well-annealed sample, the grain size tends to increase as the purity increases, so that this inequality is not so easily satisfied. Much depends in this respect on details of sample preparation, annealing sequences, etc.

We have initiated a study of grain size vs resistivity in high-purity aluminum. Some of the preliminary results are shown in Fig. 4 which is a plot of sample resistivity as a function of grain boundary area per unit sample volume. The increase in resistivity at low values of grain boundary area/unit sample volume, S/V (large grain sizes), is tentatively interpreted as release of impurities from grain boundaries which have become saturated at the minima of the curves. This is in qualitative agreement with Fig. 3 of Maimoni's paper¹⁹ where a minimum in aluminum resistivity is seen as a function of annealing temperature; he does not report the corresponding grain sizes. It is also similar to a resistivity minimum found in copper²⁰ and one in platinum²¹ as a function of annealing temperature. None of these authors have suggested an explanation of the effect.

Extrapolation of these grain-size data to other purities, cold-work and annealing sequences, etc., is complex, and we cannot yet do this with confidence. The minimum in resistivity at less than maximum annealing conditions is of considerable importance, and should influence the design and fabrication of aluminum coils.

1.B. The Lattice Resistivity

In principle there would be no resistance to the motion of conduction electrons through a perfectly regular atomic lattice if the individual atoms were rigidly fixed in position. However, rather than being fixed in position, the atoms are vibrating about their equilibrium lattice positions with an amplitude and frequency which increases as the temperature rises, and as a result there is increasing resistance to the motion of conduction electrons through the lattice. This is the cause for the rise in resistivity seen in Fig. 1 as the temperature rises above the residual resistance region.

The theory for the lattice resistivity was worked out by Grüneisen, and is covered in many texts. For a given lattice, the Debye temperature θ is an approximate characterization of the modes of vibration. Grüneisen theory predicts that

$$\begin{aligned} \rho &\propto T^5 && \text{when } T \ll \theta, \\ \text{and} &&& \\ \rho &\propto T && \text{when } T > \theta. \end{aligned}$$

For most metals, the Debye temperature is in the neighborhood of 300°K. The Debye temperature of aluminum is a little higher than most, about 400°K.^{22,23} (One must be careful to distinguish between the Debye θ evaluated from resistivity measurements and Grüneisen theory and the Debye θ evaluated from heat capacities or neutron spectroscopy. These are numerically close, but not identical.)

Numerous experiments on metals have verified that the Grüneisen theory is essentially correct, though the low temperature exponent on T is often closer to 4.5 than to 5. Several reports have shown that the lattice resistivity of aluminum at 20.4°K is about 0.64 m Ω ·cm.^{10,24-26} Of these, Pawleck and Rogalla²⁶ show that the resistivity is quite accurately proportional to T^5 from 20°K up to about 50°K, while Alexandrov and d'Yakov²⁵ obtain 4.6 as the exponent on T in this range. In the neighborhood of room temperature, the exponent on T has fallen to about 1.27.

Below 20°K, available data for aluminum by Willott,²⁷ Holwech and Jeppeson,²⁸ Alexandrov and d'Yakov,²⁵ Revel,¹⁰ and Chiang and Eremenko²⁹ are in major disagreement with extrapolation of the T^5 law as well as being generally inconsistent among each other. It happens, though, that both Revel¹⁰ and Willott²⁷ obtain a value of about 1.3×10^{-13} Ω ·m at 4.2°K. Chiang and Eremenko²⁹ mention an unpublished suggestion of Alexandrov that there is a T^2 contribution to the resistivity which is making itself felt below 20°K. Such a term has been found in transition metals and explained on the basis of electron-electron interactions,³⁰ but it is not expected to be measurable for aluminum in this purity range. A theoretical calculation by Kagan and Zhernov³¹ shows that impurities may contribute a temperature dependent resistivity. At low temperatures they calculate terms proportional to T^2 , T^4 , and T^5 , but the magnitudes of the terms are not known. At present there are no clear correlations of theory to available experimental data. We will be making resistivity measurements in this range in the near future.

Figure 5 is a graphical summary of available data on the lattice resistivity of aluminum.

1.C. The Size Effect

When an electron strikes the surface of a sample, it is reflected back into the metal in a manner which depends primarily upon its angle of incidence and the microscopic surface roughness. A certain fraction of these reflections, in particular those near grazing incidence, will be specular and have no effect on the resistivity. More generally, however, these collisions with the surface will be diffuse and add to the resistivity in the same way that collisions with impurities do. When the sample size is reduced to the point that electron collisions with the surface become comparable in frequency with other types of collisions, the resistance of the sample rises. This is called the size effect.

The natural parameter to use in evaluation of the size effect is the ratio of the sample dimension, d (thickness of plate, or diameter of wire), to the electron mean free path, ℓ , which would be observed in a large sized sample of the same percent impurity and imperfection, and at the same temperature. To evaluate ℓ , it is most convenient to make use of the equation

$$\rho \times \ell \approx \text{constant} \equiv (\rho \ell)_{\infty} , \quad (3)$$

which is approximately true for a bulk sample independent of temperature and impurity. The constant $(\rho \ell)_{\infty}$ is a measure of the area of the Fermi surface of the metal, again within a certain approximation. For aluminum, a reasonable average of reported values in the helium range is³²

$$(\rho \ell)_{\infty} \approx 0.7 \times 10^{-15} \Omega \cdot \text{m}^2 .$$

The increase in resistivity with decreasing d/ℓ was first calculated by Fuchs³³ and later Sondheimer,³⁴ on the assumption that there is no specular reflection at the surface. More recently Parrott,³⁵ and Brandli and Cotti³⁶ have extended the calculations on the assumption that electrons incident to the surface at less than some angle θ will be specularly reflected, while those incident at greater angle (more nearly normal incidence) will be diffusely reflected; the angle θ becomes an additional adjustable parameter. A yet more recent study by Soffer³⁷ relates statistical measures of surface roughness to the electron scattering process. He finds that the fractional specular reflection is angle-dependent, and that the diffuse reflection is anisotropic. The qualitative behavior of the resistivity as predicted by these theories as a function of sample thickness is shown in Fig. 6. Except for the unrealistic case of pure specular reflection, the theories are in pretty good quantitative agreement for thicknesses down to $d/\ell \approx 1$ or 2. Quantitative corrections based on Fuchs' theory for flat plates and round wires, for both dc and eddy current measurements, are given in Fig. 7. The coordinates are chosen so that a measured resistivity can conveniently be corrected to a theoretical bulk resistivity. The eddy current correction for round wires has been evaluated from an unpublished calculation provided by Dr. Cotti. For rough calculation, the size effect resistivity ρ_{SE} to be added to the bulk resistivity ρ_B is

$$\rho_{SE} \approx \frac{(\rho \ell)_{\infty}}{d} ,$$

provided $\rho_{SE} \ll \rho_B$.

2. Magnetoresistivity

The statistical link between the macroscopic electrical resistivity and the parameters describing the microscopic electron collision processes is the Boltzman equation. Its various ramifications and approximations have been the subject of much study, and

the interested reader should consult a good text if he wishes to pursue this. The point to be made here is that the presence of a magnetic field enters the Boltzman equation in such a way as to affect all the electron collision processes (except for certain special cases and approximations of no importance here). Hence the change in resistivity of a sample as a function of applied magnetic field is more generally a multiplicative factor rather than an additive factor as with Matthiessen's rule; the only exception is the size effect resistivity, as will be explained later.

The general Boltzman equation including a magnetic field is not susceptible to simple analysis. However, with certain approximations, one can obtain Kohler's rule³⁸ which is useful for engineering study:

$$\frac{\rho(H,T)}{\rho(0,T)} = f \left(\frac{H}{\rho(0,T)}, \varphi \right),$$

where φ is the angle between the field H and the measuring current. The function f is unique for a given polycrystalline metal, i.e., it is independent of small variations in purity for a nominally pure metal.

Magneto-resistance data for aluminum have been summarized by Corruccini.²⁴ For transverse magneto-resistance (field perpendicular to current), he gives an empirical equation for f which fits most available data within about $\pm 20\%$:

$$\frac{\rho(H)}{\rho(0)} - 1 = \frac{h^2 (1 + 0.00177 h)}{1.8 + 1.6 h + 0.53 h^2},$$

where

$$h \equiv H \text{ (Oe)} \times \frac{\rho_{\text{ref}}}{\rho(0)} \times 10^{-3},$$

and

$$\rho_{\text{ref}} = 2.75 \times 10^{-8} \Omega \cdot \text{m}.$$

This equation is plotted in Fig. 8. It is important to note, however, that data taken at 20°K on aluminum of 10 000 to 20 000 ratio³⁹ are in major disagreement with this curve, and show a saturation magneto-resistivity of about 7 times the zero field value, rather than the approximate value of 3 from Fig. 8. This may be an indication of temperature dependent anisotropy in the electron scattering processes, a phenomenon which was assumed not to occur in deriving Kohler's rule.

Also shown in Fig. 8 is a curve summarizing available data on the magneto-resistivity of copper.⁴⁰⁻⁴³ The linearity with field in the high field region is evident. This is related to immutable electronic properties of copper, and is the primary basis for choosing aluminum over copper for high field service.

When a sample thin enough to show the zero-field size effect is placed in an increasing magnetic field; two effects operate simultaneously: (1) The bulk resistivity begins rising as would be expected from Kohler's rule, and (2) the radius of the helical motion of the electrons decreases and for most geometries the electrons collide less often with the surface. Combination of these two effects may give resistance-field curves of unusual shape, especially in the low field region, which depend strongly on orientation.^{44,45} At sufficiently high fields the size effect resistivity often disappears.

3.A. Thermal Conductivity

The conduction of heat through a metal is governed by much the same processes which govern the flow of electric current. It turns out, in fact, that the thermal conductivity K and the electrical resistivity are quantitatively related by the Wiedemann-Franz equation

$$K \cdot \rho = L \cdot T \quad , \quad (4)$$

where L is known as the Lorenz number. Detailed theory⁴⁶ shows that in the residual resistance region at low temperatures, and at temperatures above the Debye temperature, the Lorenz number has the constant value

$$L = 2.44 \times 10^{-8} \text{ W}\Omega/\text{O.K}^2$$

for any metal or alloy in which heat transport by lattice vibrations (phonons) is negligible, i.e., for any nominally pure metal or dilute alloy. This is a very powerful result, for it allows a prediction of thermal conductivity in these two temperature ranges from much simpler measurements of electrical resistivity on the same metal.

Over the intermediate temperature range there is no simple rule, but qualitative guides can be given. Consider Eq. (4) to be exact, so that a temperature dependent Lorenz number $L(T)$ can be evaluated knowing $K(T)$ and $\rho(T)$. Generally $L(T)$ tends to drop below the theoretical value as T increases, and may exhibit less understandable bumps and dips before leveling off again at the theoretical value of $T \gg \theta$. This is illustrated in Fig. 9 (Powell, Hall, and Roder⁴⁷; these data are slightly in error at low temperatures where corrected data converge to the theoretical Lorenz number within experimental error) and Fig. 10 (Hust and Powell⁴⁸) for several aluminum alloys. Note that in no case does $L(T)$ dip below 50% of the theoretical value. It is reasonable to expect that the deviations from the theoretical value will be of this order of magnitude for other dilute alloys.

In a heavily alloyed (highly impure) sample, or in one containing many dislocations or defect structures, resistance to the motion of conduction electrons may be so high that a significant portion of the heat is carried by lattice vibrations or phonons, as with an electrical insulator. In this case, the $L(T)$ curve will rise above the theoretical value, at least initially. This is illustrated in Fig. 11 for A-110AT titanium.⁴⁸ Serious errors could occur in trying to estimate such a curve without much more knowledge than is available now.

Unfortunately there have been very few evaluations of $L(T)$ in the literature, and no detailed correlations of such curves have been made. Studies along this line have begun in our laboratory.

3.B. Thermal Conductivity in a Magnetic Field

Just as a magnetic field inhibits the flow of electric current through a metal, it also inhibits the transfer of thermal energy by the (same) conduction electrons. In a nominally pure metal or dilute alloy, where most of the heat is carried by the conduction electrons, we thus might reasonably expect that the thermal conductivity would scale with the electrical conductivity in a magnetic field. In other terms, the Lorenz number would be relatively independent of magnetic field. This topic has not been studied theoretically to my knowledge, and I have not found experimental measurements which relate directly to this suggestion, though decreasing thermal conductivity in a magnetic field has been reported.⁴⁹ This might be a deterrent to the use of copper as a thermal conductor in a high field at low temperature, because of its high magnetoresistivity.

4. Ac Effects

The response of a conductor to alternating electromagnetic fields may be typified by the relative magnitudes of three length parameters. These are:

The classical skin depth, $\delta = \left(\frac{2\rho}{\mu_0 \omega} \right)^{\frac{1}{2}}$,

The electron mean free path, ℓ ,

The sample dimension (thickness or diameter), d .

In the equation for the skin depth, ρ is the dc resistivity of a large sample of the conductor having the same percentage impurities, $\mu_0 = 4\pi \times 10^{-7}$ H/m, and ω is 2π times the frequency. If response to a pulse rather than a continuous wave is being analyzed, it will be necessary to consider the Fourier components of the pulse in order to estimate the appropriate ω and δ ; however, in some situations it may be less complicated to use other mathematical techniques which do not explicitly involve the Fourier components. Classification of the types of response is outlined in Table II and discussed below.

TABLE II
Frequency and Size Effects

$\delta > d > \ell$	dc circuit theory
$\delta > \ell > d$	dc size effect
$\ell > \delta > d$	dc size effect
$d > \delta > \ell$	classical skin effect
$d > \ell > \delta$	anomalous skin effect
$\ell > d > \delta$	"anomalous size effect"

At low frequencies $\delta > d$, current distribution is essentially uniform throughout the sample, and dc theory is applicable. If $\ell > d$, a size effect correction must be made.

When $d > \delta > \ell$, the theory of the classical skin effect applies. The current is confined to a thin surface layer, resulting in higher circuit resistance than in the dc case. The effective resistance of the surface layer is

$$Z = \left(\frac{\mu_0 \omega \rho}{2} \right)^{\frac{1}{2}}$$

When $d > \ell > \delta$, the theory of the anomalous skin effect must be used. Analysis of this situation is much more complex than that of the classical skin effect. Here the electric field sensed by an electron changes significantly over the space of one mean free path. This means that instead of using the ordinary Ohm's law $J(r) \times \rho = E(r)$ (J is the current density and E is the electric field) as was done in the classical skin effect calculation, one must in essence use an effective E averaged over the mean free path. The calculations are quite complex, and the resulting integro-differential equations have not been solved in full generality.^{46,50,51} When $\ell \gg \delta$ the resulting expression for the surface resistance is

$$Z = \left(\frac{\sqrt{3} \mu_0^2 \omega^2}{16\pi} (\rho \ell)_\infty \right)^{1/3}, \quad (5)$$

where $(\rho \ell)_\infty$ is the same fundamental parameter which arose earlier in the discussion of the dc size effect. This expression assumes 100% diffuse reflection of the electrons at the sample surface, but it is multiplied only by a factor of 8/9 if 100% specular reflection occurs. It is worth noting that in this limit the surface impedance is independent of the sample purity. The surface resistivity will be higher than that calculated from the classical skin effect, since the current density falls off more sharply with distance than in the classical case (or following Pippard's reasoning, only a fraction δ/ℓ of the electrons contribute to the effective current).

The importance of using the anomalous skin effect theory for high-purity metals can be emphasized by calculating the frequency at which the electron mean free path ℓ is equal to the classical skin depth δ . Calling this frequency ω_c , we find

$$\omega_c = \frac{2\rho^3}{\mu_0 (\rho \ell)_\infty^2}$$

For aluminum this turns out to be a frequency

$$f_c \text{ (Hz)} = \frac{\omega_c}{2\pi} \approx \frac{10}{\left(\frac{\text{r.r.}}{10^4}\right)^3},$$

where r.r. is the resistivity ratio, $2.64 \mu\Omega \cdot \text{cm}/\rho$. Aluminum can be purchased at the present time in large ingots of about 14 000 resistivity ratio. With this material at helium temperatures, the anomalous skin effect theory would be necessary above about 4 Hz; with the most pure aluminum obtained in the laboratory (45 000 ratio), the anomalous skin effect theory would be used above 0.1 Hz.

When $\ell > d > \delta$, the theory of the anomalous skin effect must be combined with the size effect calculation. This subject has been discussed in the literature (Gantmakher⁵² and references cited therein), though with particular application to various cyclotron-like resonances which occur in single crystals in a large static magnetic field. The analysis is not particularly applicable to systems in the absence of a magnetic field, and it is not clear what modification would be necessary in Eq. (5), for example. Cotti's eddy-current size effect correction illustrated in Fig. 7 is somewhat related to this problem, but his analysis was made in terms of response to a step function and did not treat individual Fourier components.

5. Summary

Through the analysis of Section 1, the complete resistivity-temperature curve for aluminum may be constructed by adding the residual resistivity to the "lattice" resistivity. The residual resistivity may be determined by direct measurement, or estimated from knowledge of impurity content, grain size, and state of lattice strain. The "lattice" resistivity below 20°K is not known accurately, but the curve in Fig. 5 labeled "Alexandrov" is probably the best estimate at the present time. The resistivity in a magnetic field at any temperature may then be calculated from the Kohler plot in Fig. 8; the important discrepancy between this curve and the data of Borovik, Volotskaya, and Fogel³⁹ for aluminum of the highest purity around 20°K is unresolved at present.

The thermal conductivity at any temperature may then be estimated from the Wiedemann-Franz relationship, Eq. (4), knowing the resistivity and assuming that the Lorenz number is roughly constant. More accurate assumptions on the Lorenz number are possible, in keeping with the curves of Figs. 9 and 10, but insufficient data exist to establish a truly reliable $L(T)$ curve for high purity aluminum. Though the derivation of the Lorenz number assumed the absence of a magnetic field, it is postulated that in the first approximation the Lorenz number would be independent of magnetic field. Thus the thermal conductivity should decrease as the electrical resistivity increases.

The response of a conductor to alternating electromagnetic fields is discussed in terms of the skin depth δ , the electron mean free path ℓ , and the sample dimension d . The importance of the anomalous skin effect theory for high purity metals at low temperatures is emphasized. Calculations based on this theory are very complex, and have not been carried out except for the limiting case $d \gg \ell \gg \delta$, in which case the surface resistivity becomes independent of sample purity. In any case the surface resistivity will be higher than that calculated by the classical skin effect theory, since (in one sense) not all the electrons can effectively respond to the applied field.

III. PREPARATION OF HIGH-PURITY ALUMINUM

Since the first separation of the metal from its ore, aluminum has been prepared by electrolytic reduction of molten aluminum oxide. Ishihara and Mukai⁵³ have suggested that residual impurities in the aluminum produced by this process may be strongly influenced by contaminants in the carbon electrodes, as well as the impurities in the original ore. With very careful selection, it is possible to obtain multikilogram quantities refined by only this technique having resistivity ratios in the range 1000 to 2000.

To obtain additional purity, zone refining is performed on the nominally pure metal. This process is usually found only on the laboratory scale, producing at most perhaps one-kilogram ingots at a low rate. Recently, however, a commercial source of zone refined ingots weighing up to about 40 kg has become available. The best 20 kg of these ingots are apparently of reasonably uniform high purity, having resistivity ratios in the 13 000 to 17 000 range. This seems to open the door to possible technological use in large-scale applications. We have found that this material can be handled and shaped, on a laboratory scale at least, without measurable contamination.

The success of zone refining depends on the increased solubility of impurity atoms in the molten metal as compared to their solubility in the solid. It turns out for aluminum⁵⁴ that Mn has close to the same solubility in the solid as in the liquid, while Ti, V, Cr, Zr, Nb, Mo, Ta, and W are less soluble in the liquid than in the solid. These are the impurities, then, which are not easily removed by zone refining, so that the final purity is significantly limited by the initial presence of these particular elements.

It seems clear that careful selection, probably including the source of the ore, may measurably improve the final product. Research groups in Norway, France, and Russia have reported zone refined aluminum, presumably in small quantities, having resistivity ratios in the 22 000 to 29 000 range.^{39,55,56} Dr. Bratsberg has indicated to us (private correspondence) that the choice of starting material is of great importance.

The French group^{57,58} has carried this line of reasoning one step further. They have obtained small quantities of aluminum prepared by an "organic refining" process involving the electrolytic reduction of $Al(C_2H_5)_3$ and/or related compounds. This produces aluminum of 8000 to 10 000 ratio. With subsequent zone refining of this material,

Revel has obtained a resistivity ratio of 39 000 on a 5 mm diameter sample; correcting for the size effect, this corresponds to a resistivity ratio of about 47 000 for a bulk specimen. We likewise have obtained a small quantity of the organically-refined aluminum, had it zone refined, and obtained a resistivity ratio of about 45 000; correcting for the size effect in our sample brings this to 47 000, in remarkable agreement with the ratio obtained by Dr. Revel. We speculate that this organic refining method happens to be relatively effective in removing the transition metals which cannot easily be extracted by zone refining. We are having mass spectroscopic analyses made to cover this point, but do not yet have the results.

The availability of commercial quantities of this "organically-refined" aluminum seems remote at this time. The process is slow, and the high-purity anode decomposes at a relatively fast rate. Aluminum triethylene reacts vigorously or explodes on contact with oxygen, hydrogen, phenol, alcohol, acids, and water, and explodes spontaneously above 180°C. The reactivity can be lessened somewhat by addition of related organic compounds, but apparently this involves compensating disadvantages in the refining process.

At this time, then, it seems that for design purposes one can count on availability of about 15 000-ratio aluminum in ingots of about 20 kg. For laboratory measurements, one can obtain small quantities of about 45 000-ratio aluminum, but a major technological development would be required to obtain this on a commercial scale.

ACKNOWLEDGEMENTS

M.B. Kasen and R.P. Reed have contributed significantly to the collection and analysis of stress, strain, grain size, and annealing temperature effects in aluminum. More complete data and analysis will be published elsewhere. R.H. Kropschot has given valuable encouragement and advice, particularly with reference to possible technological usage. The work has been supported in part by contract LB523801A308 with the Army Missile Command, and in part by contract F33615-68-M-5000 with Wright-Patterson Air Force Base.

REFERENCES

1. R.F. Post and C.E. Taylor, in Advances in Cryogenic Engineering (Plenum Press, 1959), Vol. 5, p. 13.
2. J.R. Purcell and E.G. Payne, *Rev. Sci. Instr.* 34, 893 (1963).
3. V. Arp, in Proc. Intern. Symposium Magnet Technology, Stanford, 1965, p. 625.
4. C.E. Oberly and R.R. Barthelemy, in Proc. 12th Intern. Congress on Refrigeration, Madrid, Spain, 1967, Paper No. I.27.
5. R.L. Powell, H.M. Roder, and W.J. Hall, *Phys. Rev.* 115, 314 (1959).
6. L.A. Hall, National Bureau of Standards Technical Note 365 (1968).
7. C.R. Vassel, *J. Phys. Chem. Solids* 7, 90 (1958).
8. E. Kovacs-Csetenyi, C.R. Vassel, and I. Kovacs, *Phys. Stat. Sol.* 17, 123 (1966).
9. G. Boato, M. Bugo, and C. Rizzuto, *Nuovo Cimento* 45, 226 (1966).
10. G. Revel, *Mem. Sci. Rev. Met.* 65, 181 (1968).
11. J.J. Gniewek and A.F. Clark, *J. Appl. Phys.* 36, 3358 (1965).
12. R.M.J. Cotterill, *Phil. Mag.* 8, 1937 (1963).
13. Z.S. Basinski and S. Saimoto, *Can. J. Phys.* 45, 1161 (1967).

14. V. Ya. Kravchenko, Soviet Phys. - Solid State 9, 653 (1967).
15. H. Maeta, J. Phys. Soc. Japan 24, 757 (1968).
16. J.G. Rider and C.T.B. Foxon, Phil. Mag. 13, 289 (1966).
17. H.G. Van Bueren, Imperfections in Crystals (North-Holland Publishing Co., 1960).
18. D. McLean, Grain Boundaries in Metals (Clarendon Press, 1957).
19. A. Maimoni, Cryogenics 2, 217 (1962).
20. P.V. Andrews, Phys. Letters 19, 558 (1965).
21. K. Misec, Czech J. Phys. B17, 647 (1967).
22. V.P. Varshni and R.C. Shukula, J. Chem. Phys. 43, 3966 (1965).
23. R. Stedman, L. Almquist, and G. Nilsson, Phys. Rev. 162, 549 (1967).
24. R.J. Corruccini, National Bureau of Standards Technical Note No. 218 (1964).
25. B.N. Aleksandrov and I.G. d'Yakov, Soviet Phys. - JETP 16, 603 (1963).
26. F. Pawleck and D. Rogalla, Metall. und Tech. 20, 949 (1966).
27. W.B. Willott, Phil. Mag. 16, 691 (1967).
28. I. Holwech and J. Jeppesen, Phil. Mag. 15, 217 (1967).
29. Yu. N. Chiang and V.V. Eremenko, Soviet Phys. - JETP Letters 3, 293 (1966).
30. M.J. Rice, Phys. Rev. Letters 20, 1439 (1968).
31. Yu. Kagan and A.P. Zhernov, Soviet Phys. - JETP 23, 737 (1966).
32. P. Cotti, E.M. Fryer, and J.L. Olsen, Helv. Phys. Acta 37, 585 (1964).
33. K. Fuchs, Proc. Cambridge Phil. Soc. 34, 100 (1938).
34. E.H. Sondheimer, Advan. Phys. 1, 1 (1952).
35. J.E. Parrott, Proc. Phys. Soc. (London) 85, 1143 (1965).
36. G. Brandli and P. Cotti, Helv. Phys. Acta 38, 801 (1965).
37. S.B. Soffer, J. Appl. Phys. 38, 1710 (1967).
38. M. Kohler, Ann. Physik 32, 211 (1938).
39. E.S. Borovik, V.G. Volotskaya, and N. Ya. Fogel, Soviet Phys. - JETP 18, 34 (1964).
40. International Copper Research Association, unpublished, 1968.
41. G. Yntema, Phys. Rev. 91, 1953).
42. T.G. Berlincourt, Phys. Rev. 112, 381 (1958).
43. B. Luthi, Helv. Phys. Acta 33, 161 (1960).
44. B.N. Aleksandrov, Soviet Phys. - JETP 16, 286 (1963).
45. K. Forsvoll and I. Holwech, J. Appl. Phys. 34, 2230 (1963).
46. J.M. Ziman, Electrons and Phonons (Clarendon Press, 1960).
47. R.L. Powell, W.J. Hall, and H.M. Roder, J. Appl. Phys. 31, 496 (1960).
48. J.G. Hust and R.L. Powell, private communication (1968).
49. T. Amundsen and T. Olsen, Phys. Letters 4, 304 (1963).
50. A.B. Pippard, Rept. Progr. Phys. 22, 176 (1960).
51. G.E. Smith, in The Fermi Surface, edited by W.A. Harrison and M.B. Webb (J. Wiley & Sons, 1960).

52. V.F. Gantmakher, in Progress in Low Temperature Physics, edited by C.J. Gorter (North-Holland Publishing Co., 1967), Vol. 5, p. 181.
53. M. Ishihara and K. Mukai, Trans. AIME 236, 192 (1966).
54. G. Revel, Thesis (unpublished), 1965.
55. F. Montariol and R. Reich, Compt. Rend. 254, 3535 (1962).
56. H. Bratsberg, D. Foss, and O.H. Herbjornsen, Rev. Sci. Instr. 34, 777 (1963).
57. J. Bonmarin, Rev. Aluminum 330, 455 (1965).
58. G. Revel, Ann. Chim. (Paris) 1, 37 (1966).

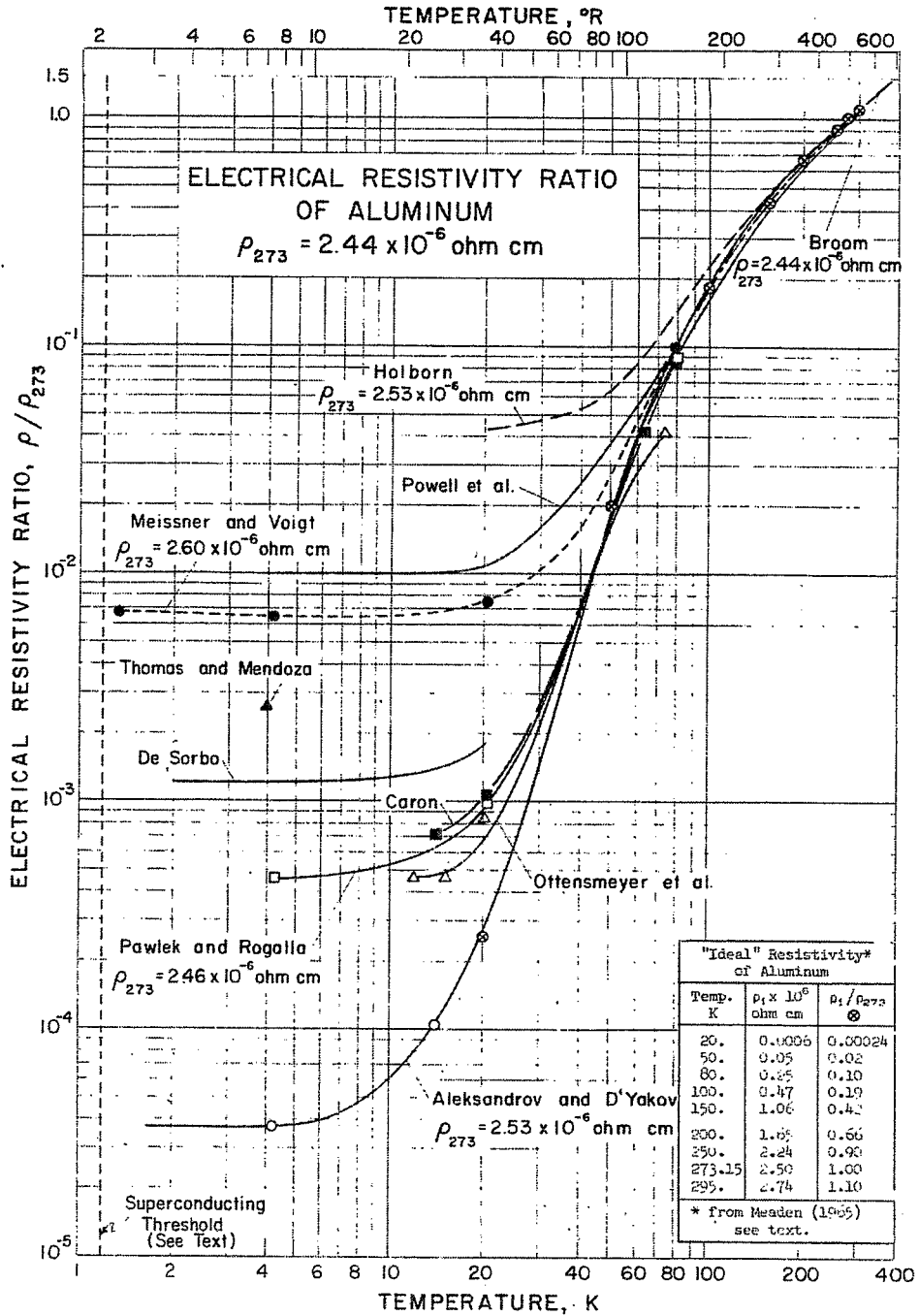


Fig. 1. Compilation of electrical resistivity measurements on aluminum.

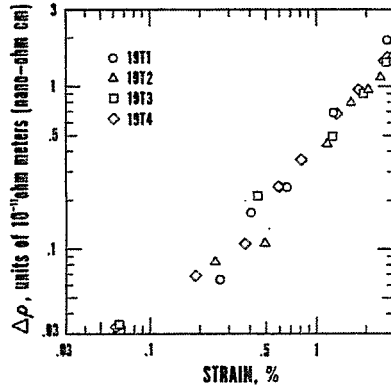


Fig. 2. Strain-induced resistivity in 2000-ratio aluminum at 4°K.

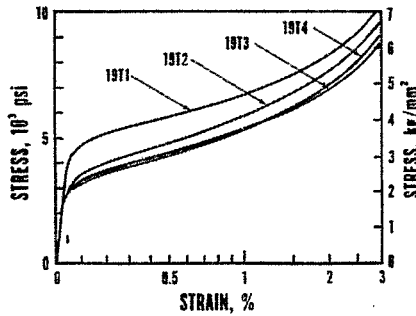


Fig. 3. Stress as a function of strain in polycrystalline 2000-ratio aluminum at 4°K. Data taken simultaneously with that of Fig. 2.

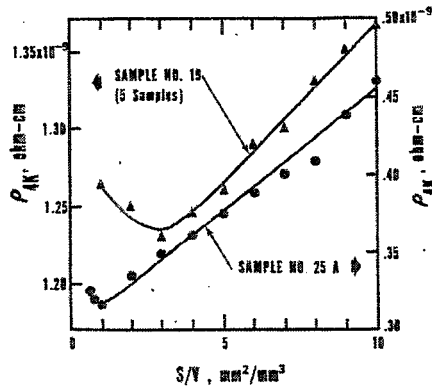


Fig. 4. Resistivity at 4°K as a function of grain boundary area per unit sample volume for two different sample purities. All five of the No. 19 samples had very close to the same purity.

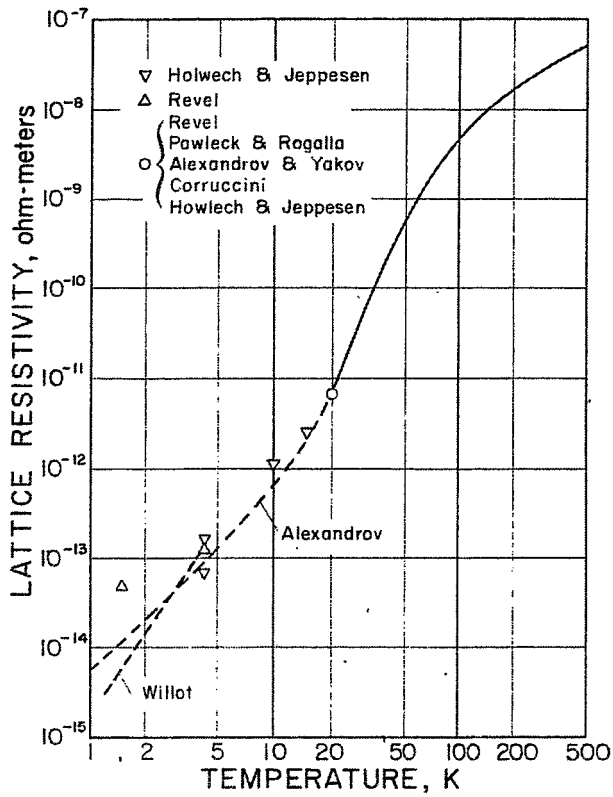


Fig. 5. Lattice resistivity of aluminum as a function of temperature.

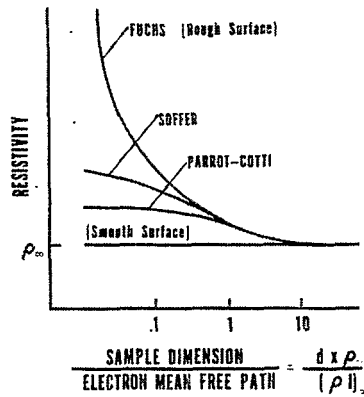


Fig. 6. Qualitative behavior of the resistivity as a function of (sample size/electron mean free path), according to various size effect theories.

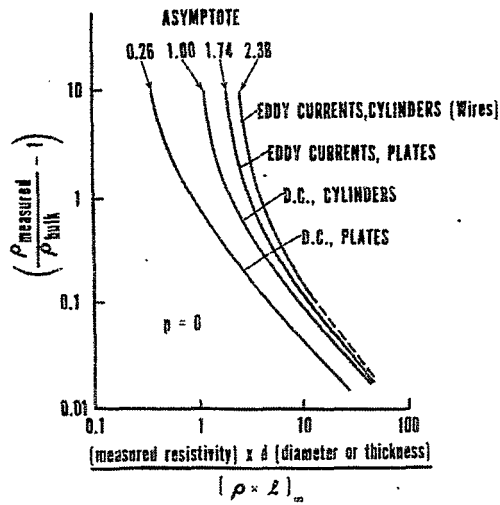


Fig. 7. The size effect correction assuming 100% diffuse reflection of electrons at the sample surface. These are equivalent to the "Fuchs" curve in Fig. 6.

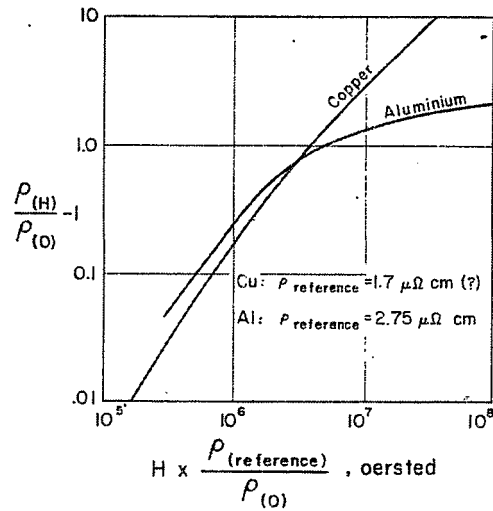


Fig. 8. Kohler plot giving transverse magnetoresistance of copper and aluminum.

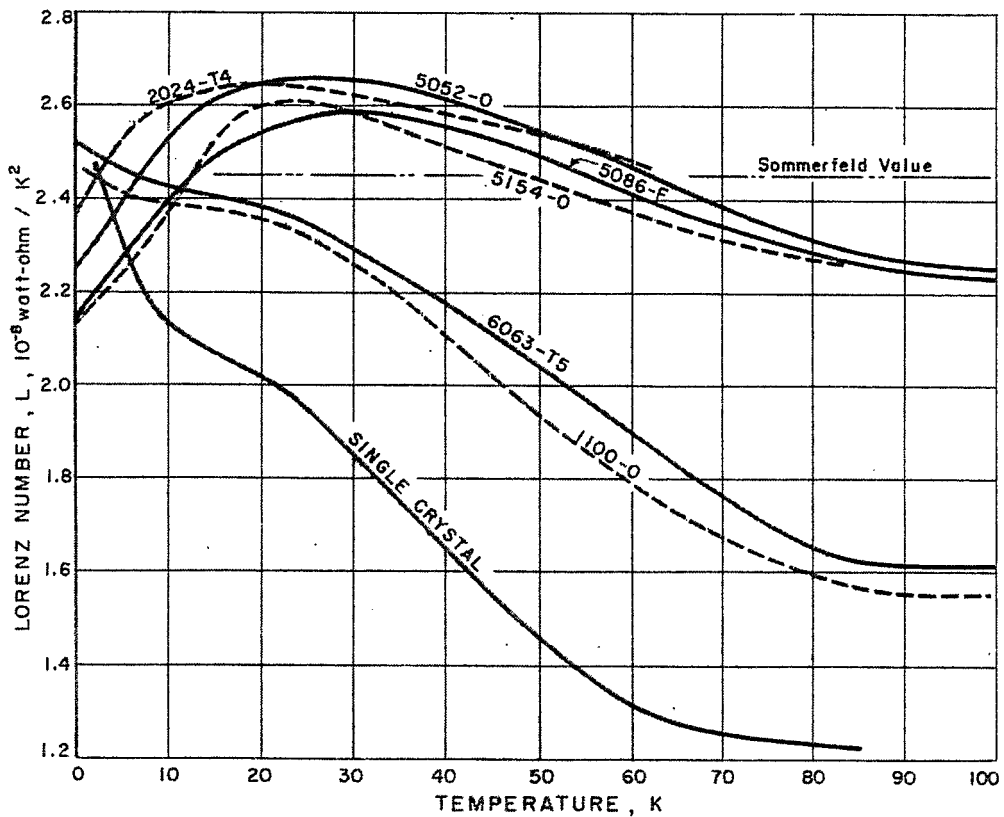


Fig. 9. Lorenz number as a function of temperature for several aluminum alloys. (The data actually converge the theoretical value 2.44×10^{-8} as $T \rightarrow 0$; the graph is slightly in error due to a calibration error.)

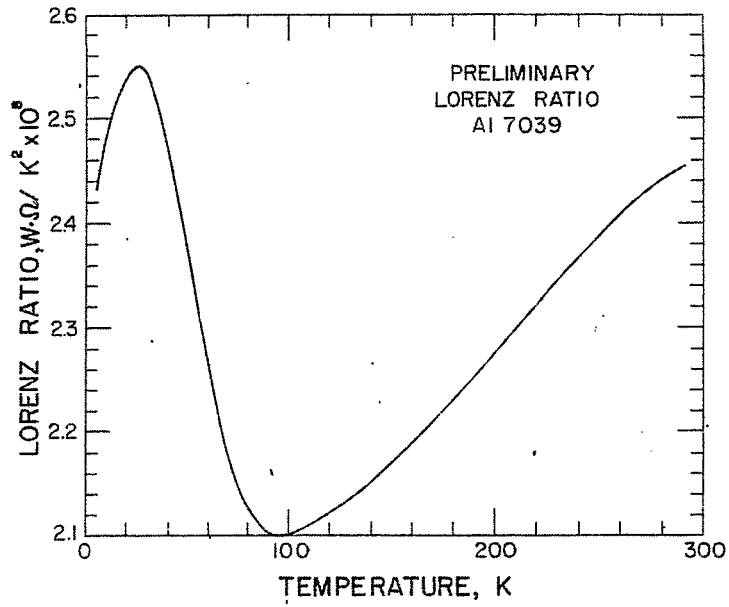


Fig. 10. Lorenz number as a function of temperature for 7039 aluminum.

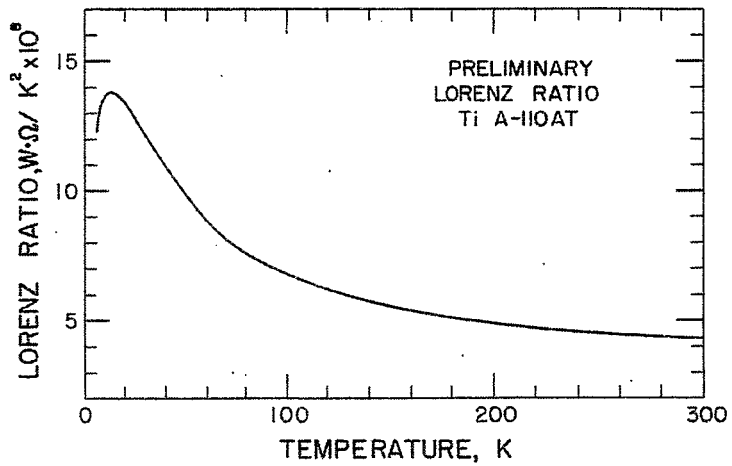


Fig. 11. Lorenz number as a function of temperature for A-110AT titanium alloy.